Inorg. Chem. **2007**, *46*, 3593–3602

Molecular Recognition of Adeninium Cations on Anionic Metal–Oxalato Frameworks: An Experimental and Theoretical Analysis

Juan P. García-Terán, Oscar Castillo,* Antonio Luque,* Urko García-Couceiro, Garikoitz Beobide, and Pascual Román

Departamento de Química Inorgánica, Facultad de Ciencia y Tecnología, Universidad del País Vasco, Apartado 644, E-48080 Bilbao, Spain

Received December 21, 2006

Reactions of adenine with water-soluble oxalato complexes at acidic pH give the compounds (1*H*,9*H*-ade)$_2$[Cu(ox)$_2$(H$_2$O)] (**1**) [H$_2$ade = adeninium cation (1+), ox = oxalato ligand (2–)] and (3*H*,7*H*-ade)$_2$[M(ox)$_2$(H$_2$O)$_2$]·2H$_2$O [M(II) = Co (**2**), Zn (**3**)]. The X-ray single crystal analyses show that the supramolecular architecture of all compounds is built up of anionic sheets of metal–oxalato–water complexes and ribbons of cationic nucleobases among them to afford lamellar inorganic–organic hybrid materials. The molecular recognition process between the organic and the inorganic frameworks determines the isolated tautomeric form of the adeninium cation found in the crystal structures: the canonical 1*H*,9*H* for compound **1**, and the first solid-state characterized 3*H*,7*H*-adeninium tautomer for compounds **2** and **3**. Density functional theory calculations have been performed to study the stability of the protonated nucleobase forms and their hydrogen-bonded associations by comparing experimental and theoretical results.

Introduction

The elucidation of the DNA double-stranded helix by Watson and Crick[1] represented not only a breakthrough in the structural biology[2] but also the starting point for the appealing and flourishing research dedicated to the rational design and elaboration of biomimetic systems based on the interaction of DNA/RNA constituents and their derivatives with an extensive range of both organic and inorganic frameworks.[3] The driving force of these multidisciplinary studies has been to gain a wealth of knowledge which helps to deepen the understanding of a great diversity of molecular biorecognition processes and to offer a powerful tool for the efficient synthesis of advanced functional materials with tailor-made properties and potential applications for the material sciences[4] and the therapeutic medicine.[5]

A particular aspect of the nucleobase behavior that has attracted growing attention in recent years is the influence of metal ions[6,7] and hydrogen bond donor/acceptors (solvent and small molecules)[8] on the tautomeric and protonation equilibria of nucleic acid bases. Chemical reactions that involve single- or multiple-proton transfers are responsible for numerous examples of homo- and heterobases mispairing which, if undetected by repair enzymes, could lead to a point mutation in the genome,[9] but they also afford noncanonical tautomers and protonated forms which seem to play a crucial role in the high degree of photostability of the nucleobases, essential to protect life on earth from the DNA/RNA damage

* To whom correspondence should be addressed. E-mail: oscar.castillo@ehu.es (O.C.), antonio.luque@ehu.es (A.L.).

(1) Watson, J. D.; Crick, F. H. C. *Nature* **1953**, *171*, 737.
(2) (a) *Oxford Handbook of Nucleic Acid Structure*; Neidle, S., Ed.; Oxford University Press: Oxford, 1999. (b) *Nucleic Acids in Chemistry and Biology*; Blackburn, G. M., Gait, M. J., Eds.; Oxford University Press: Oxford, 1996.
(3) (a) Sivakova, S.; Rowan, S. J. *Chem. Soc. Rev.* **2005**, *34*, 9. (b) Derose, V. J.; Burns, S.; Kim, N. K.; Vogt, M. In *Comprehensive Coordination Chemistry II*; McCleverty, J. A., Meyer, T. J., Eds.; Elsevier: University of Bern, Switzerland, 2004; Vol. 8, pp 787−813. (c) Navarro, J. A. R.; Lippert, B. *Coord. Chem. Rev.* **2001**, *222*, 219. (d) Lippert, B. *Coord. Chem. Rev.* **2000**, *200*−*202*, 487.
(4) (a) Simmel, F. C.; Yurke, B. In *Encyclopedia of Nanoscience and Nanotechnology*; Nalwa, H. S., Ed.; American Scientific Publishers: 2004; Vol. 2, pp 495−504. (b) Santoso, S. S.; Zhang, S. In *Encyclopedia of Nanoscience and Nanotechnology*; Nalwa, H. S., Ed.; American Scientific Publishers: 2004; Vol. 9, pp 459−471. (c) Gottarelli, G.; Masiero, S.; Mezzina, E.; Spada, G. P.; Mariani, P.; Recanatini, M. *Helv. Chim. Acta* **1998**, *81*, 2078.
(5) (a) Natile, G.; Marzilli, L. G. *Coord. Chem. Rev.* **2006**, *250*, 1315. (b) Erkkila, K. E.; Odom, D. T.; Barton, J. K. *Chem. Rev.* **1999**, *99*, 2777.
(6) Lippert, B. In *Progress in Inorganic Chemistry*; Karlin, K. D., Ed.; John Wiley and Sons: New York, 2005; Vol. 54, pp 385−447.
(7) Sigel, H. *Pure Appl. Chem.* **2004**, *76*, 1869.
(8) McConnell, T. L.; Wheaton, C. A.; Hunter, K. C.; Wetmore, S. D. *J. Phys. Chem. A* **2005**, *109*, 6351.
(9) Gorb, L.; Podolyan, Y.; Dziekonski, P.; Sokalski, W. A.; Leszczynski, J. *J. Am. Chem. Soc.* **2004**, *126*, 10119.

10.1021/ic062448s CCC: $37.00
Published on Web 03/22/2007

Scheme 1

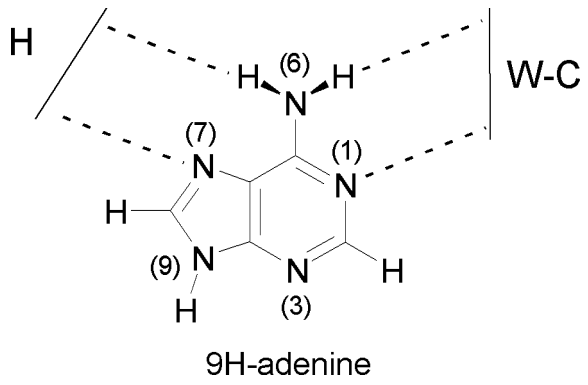

9H-adenine

from the UV irradiation of sunlight.[10] Protonated nucleobases are present in many biochemical processes (i.e., enzymatic reactions, stabilization of triplex structures), and they play a key role in a newly emerging feature of nucleic acid chemistry, namely, acid−base catalysis.[6]

Adenine offers five available proton attachment sites (Scheme 1, basicity order: N9 > N1 > N7 > N3 > N6-exocyclic) which provide it the widest range of neutral tautomers and protonated forms, and it has been the subject of numerous theoretical[11,12] and experimental investigations.[10] Most of the studies concerning DNA/RNA nucleobases have been realized in the gas phase[13,14] or aqueous media,[15] but notable advances have been made in solid-state chemistry such as (without being exhaustive) (a) the construction of nanobiological devices,[16] (b) the design and improvement of chemical-biology tools and/or pharmaceutical agents,[17] (c) the stabilization of noncanonical tautomers through interactions with metallic ions[18] and/or hydrogen bonding donor/acceptor species,[19] and (d) the building of high dimensional covalent architectures containing nucleobases as bridging or terminal ligands.[20−22]

In this area, our group has recently reported the structural and magnetic characterization of the first covalent 3D network containing adenine as bridging ligand, the porous coordination polymer $\{[Cu_2(\mu\text{-ade-}\kappa^3\text{-}N3,N7,N9)_4(H_2O)_2][Cu(ox)(H_2O)]_2\cdot\sim 14H_2O\}_n$,[22] and the first examples of one-dimensional polymeric complexes containing a natural DNA purine nucleobase as peripheral ligand.[21] Recently, our synthesis efforts have been successful with the unprecedented solid-state characterization of the minor 7*H*-adenine tautomer as free molecule (without metal coordination) stabilized through a strong network of hydrogen-bonding interactions involving the manganese−oxalato framework of the complex $\{[Mn(\mu\text{-ox})(H_2O)_2](7H\text{-ade})\cdot(H_2O)\}_n$.[19] Until then, noncanonical adenine tautomers had been found in compounds where the proton transfer is brought about by a synergy of metal coordination to the N9 donor site and an efficient stabilization of the resulting tautomeric form by noncovalent interactions.[18]

Scheme 2

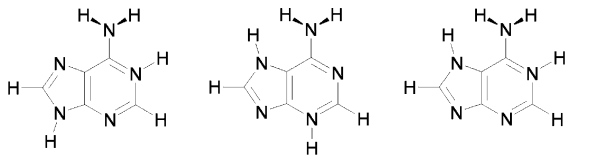

1H,9H-adeninium 3H,7H-adeninium 1H,7H-adeninium

Following our current program on molecular recognition processes between nucleobases and metal−oxalato frameworks, we report herein the synthesis and supramolecular architectures of the compounds $(1H,9H\text{-ade})_2[Cu(ox)_2(H_2O)]$ (**1**) and $(3H,7H\text{-ade})_2[M(ox)_2(H_2O)_2]\cdot 2H_2O$ [M(II) = Co (**2**), Zn (**3**)]. Of particular note is the fact that compound **1** presents the twofold protonated 1*H*,9*H*-adeninium cation (Scheme 2) in agreement with the relative basicity of the N-rich nucleobase (N9 > N1 > N7 > N3 > N6-exocyclic) but compounds **2** and **3** contain an unexpected cation having hydrogen atoms at N3 and N7, which is unprecedented in the adenine solid-state chemistry. Although the 3*H*,7*H*-adeninium entity has been postulated as the second most stable protonated form of adenine (0.46 kcal/mol above the lowest-energy 1*H*,9*H*-adeninium form)[23] by means of density functional theory calculations, by our knowledge, it has not been crystallographically (in solid-state form) characterized so far.

Experimental Section

Materials and Physical Measurements. Standard literature procedures were used to prepare the starting materials $K_2[Cu(ox)_2]\cdot 2H_2O$, $[Co(\mu\text{-ox})(H_2O)_2]_n$, and $[Zn(\mu\text{-ox})(H_2O)_2]_n$.[24] Elemental

(10) (a) Crespo-Hernandez, C. E.; Cohen, B.; Hare, P. M.; Kohler, B. *Chem. Rev.* **2004**, *104*, 1977. (b) Chen, H.; Shuhua, L. *J. Phys. Chem. A* **2005**, *109*, 8443.
(11) Sponer, J.; Leszczynski, J.; Hobza, P. *Biopolymers* **2002**, *61*, 2002.
(12) Turecek, F.; Chen, X. *J. Am. Soc. Mass Spectrom.* **2005**, *16*, 1713.
(13) Fonseca-Guerra, C.; Bickelhaupt, F. M.; Saha, S.; Wang, F. *J. Phys. Chem. A* **2006**, *110*, 4012.
(14) Vrkic, A. K.; Taverner, T.; James, P. F.; O'Hair, A. J. *Dalton Trans.* **2004**, 197.
(15) Hanus, M.; Kabelac, M.; Rejnek, J.; Ryjacek, F.; Hobza, P. *J. Phys. Chem. B* **2004**, *108*, 2087.
(16) (a) Lee, S. C.; Ruegsegger, M. A.; Ferrari, M. In *Encyclopedia of Nanoscience and Nanotechnology*; Nalwa, H. S., Ed.; American Scientific Publishers: 2004; Vol. 1, pp 309−327. (b) Mezzina, E.; Mariani, P.; Itri, R.; Masiero, S.; Pieraccini, S.; Spada, G. P.; Spinozzi, F.; Davis, J. T.; Gottarelli, G. *Chem. Eur. J.* **2001**, *7*, 388.
(17) Legraverend, M.; Grierson, D. S. *Bioorg. Med. Chem.* **2006**, *14*, 3987.
(18) (a) Suzuki, T.; Hirai, Y.; Monjushiro, H.; Kaizaki, S. *Inorg. Chem.* **2004**, *43*, 6435. (b) Rojas-González, P. X.; Castiñeiras, A.; González-Pérez, J. M.; Choquesillo-Lazarte, D.; Niclós-Gutiérrez, J. *Inorg. Chem.* **2002**, *41*, 6190. (c) Sheldrick, W. S.; Hagen-Eckhard, H. S.; Hebb, S. *Inorg. Chim. Acta.* **1993**, *206*, 15. (d) Zamora, F.; Kunsman, M.; Sabat, M.; Lippert, B. *Inorg. Chem.* **1997**, *36*, 1583.
(19) García-Terán, J. P.; Castillo, O.; Luque, A.; García-Couceiro, U.; Beobide, G.; Román, P. *Dalton Trans.* **2006**, 902.
(20) (a) González-Pérez, J. M.; Alarcón-Payer, C.; Castiñeiras, A.; Pivetta, T.; Lezama, L.; Choquesillo-Lazarte, D.; Crisponi, G.; Niclós-Gutiérrez, J. *Inorg. Chem.* **2006**, *45*, 877. (b) Purohit, C. S.; Verma, S. *J. Am. Chem. Soc.* **2006**, *128*, 400. (c) Olea, D.; Alexandre, S. S.; Amo-Ochoa, P.; Guijarro, A.; de Jesús, F.; Soler, J. M.; de Pablo, P. J.; Zamora, F.; Gomez-Herrero, J. *Adv. Mater.* **2005**, *17*, 1761. (d) Das, S.; Madhavaiah, C.; Verma, S.; Bharadwaj, P. K. *Inorg. Chim. Acta* **2005**, *358*, 3236.
(21) García-Terán, J. P.; Castillo, O.; Luque, A.; García-Couceiro, U.; Román, P.; Lloret, F. *Inorg. Chem.* **2004**, *43*, 5761.
(22) García-Terán, J. P.; Castillo, O.; Luque, A.; García-Couceiro, U.; Román, P.; Lezama, L. *Inorg. Chem.* **2004**, *43*, 4549.
(23) Marian, C.; Nolting, D.; Weinkauf, R. *Phys. Chem. Chem. Phys.* **2005**, *7*, 3306.
(24) (a) Remy, H. In *Treatise on Inorganic Chemistry*; VCH: Weinheim, Germany, 1956. (b) Kirschner, S. In *Inorganic Synthesis*; Rochow, E. G., Ed.; McGraw-Hill Book Co.: New York, 1960; Vol. VI.

Table 1. Single-Crystal Data and Structure Refinement Details for Compounds **1**−**3**[a]

	1	**2**	**3**
empirical formula	$C_{14}H_{14}CuN_{10}O_9$	$C_{14}H_{20}CoN_{10}O_{12}$	$C_{14}H_{20}N_{10}O_{12}Zn$
M_r	529.89	579.33	585.79
cryst syst	triclinic	monoclinic	monoclinic
space group	$P\bar{1}$	$C2/c$	$C2/c$
a/Å	8.960(5)	24.549(5)	24.653(4)
b/Å	10.104(5)	7.631(1)	7.626(1)
c/Å	11.403(4)	12.752(3)	12.782(3)
α/deg	103.96(4)	90	90
β/deg	103.68(4)	114.91(2)	115.44(2)
γ/deg	104.94(5)	90	90
V/Å^3	917.6(9)	2166.6(8)	2170.1(8)
Z	2	4	4
D_c/Mg·m^{-3}	1.918	1.776	1.793
color	light blue	pink	colorless
cryst habit	prismatic	prismatic	prismatic
cryst size/mm^3	0.05 × 0.03 × 0.02	0.32 × 0.19 × 0.12	0.08 × 0.05 × 0.04
μ/mm^{-1}	1.273	0.881	1.220
$2\theta_{max}$/deg	56.10	56.08	56.28
reflns collected	7974	5180	5112
indep reflns	4409	2607	2610
R_{int}	0.0949	0.0451	0.0657
variable params	307	169	169
R1/wR2[a]	0.0495/0.0784	0.0681/0.1778	0.0747/0.1971
GOF (F^2)	0.910	1.184	1.040
$\Delta\rho_{max/min}$/e Å^{-3}	0.578, −0.338	1.233, −0.380	1.550, −0.390

[a] $R1 = \Sigma||F_o| - |F_c||/\Sigma|F_o|$; $wR2 = [\Sigma[w(F_o^2 - F_c^2)^2]/[\Sigma(F_o^2)^2]]^{1/2}$ where $w = 1/[\sigma^2(F_o^2) + (AP)^2 + (BP)]$ with $A = 0$ (**1**), 0.0595 (**2**), 0.0941 (**3**), and $B = 11.2765$ (**1**), 11.2765 (**2**), 6.0438 (**3**).

analyses (C, H, N) were performed on a Perkin-Elmer 2400 microanalytical analyzer. Metal content was determined by absorption spectrometry. The IR spectra (KBr pellets) were recorded on a FTIR Mattson 1000 spectrometer in the 4000−400 cm^{-1} spectral region.

Preparations. (1*H*,9*H*-ade)$_2$[Cu(ox)$_2$(H$_2$O)] [1]. An aqueous-methanol solution (16 mL, 1/1 ratio) of adenine (0.057 g, 0.42 mmol) was added dropwise to an aqueous solution (10 mL) of K_2-[Cu(ox)$_2$]·2H$_2$O (0.050 g, 0.14 mmol) and K$_2$(ox)·H$_2$O (0.026 g, 0.14 mmol) with continuous stirring at 50 °C. Light-blue crystals of compound **1** were obtained by the slow diffusion of this mixture into an aqueous solution of 0.1 M HNO_3. Crystal growth was observed after three weeks. Yield: 30−40% (based on metal). Found: C, 31.94; H, 2.53; N, 26.64; Cu, 12.08. $C_{14}H_{14}CuN_{10}O_9$ requires C, 31.73; H, 2.66; N, 26.43; Cu, 11.99%. FT-IR ν_{max}(KBr pellet)/cm^{-1}: 3452s ν(O−H); 3242s (ν(NH$_2$) + 2δ(NH$_2$)); 3071s (ν(C$_8$−H + C$_2$−H) + (ν(NH$_2$)); 1688sh, 1674vs n$_{as}$ (O−C−O); 1600s (ν(C═C) + δ(NH$_2$)); 1516w (ν(C$_4$−C$_5$) + (N$_3$−C$_4$−C$_5$)); 1481w, 1450w (δ(C$_2$−H + C$_8$−N$_9$) + ν(C$_8$−H)); 1414s δ(N$_1$−C$_6$−H$_6$); 1383s ν(C$_5$−N$_7$−C$_8$); 1299 w, 1273s (ν(N$_9$−C$_8$ + N$_3$−C$_2$) + δ(C−H) + ν_s(O−C−O)); 1245 m, 1206 m, 1137w (δ(C$_8$−H) + ν(N$_7$−C$_8$)); 1102w, 1035w τ(NH$_2$); 939 m, 900w, 887w (ν(N$_1$−C$_6$) + τ(NH$_2$)); 799s, δ(O−C−O); 714s, 683m, 639m, 615m (ring deformation); 558m, 536m, 520m, 489m ν(M−O).

(3H,7H-ade)$_2$[Co(ox)$_2$(H$_2$O)$_2$]·2H$_2$O (2). An aqueous-methanol solution (16 mL, 1/1 ratio) of adenine (0.057 g, 0.42 mmol) was added dropwise to an aqueous mixture (15 mL) of [Co(μ−ox)-(H$_2$O)$_2$] (0.026 g, 0.14 mmol) and K$_2$(ox)·H$_2$O (0.156 g, 0.85 mmol) with continuous stirring at 50 °C. The resulting solution (pH = 7.0), was acidified with $H_2C_2O_4$ 0.1 M up to a pH value of 4.5 where a muddy solution was formed. The solution was filtered and left to evaporate slowly at room temperature. In a period of 2−4 days, X-ray quality pink crystals were grown. Yield: 30−40%. Found: C, 29.06; H, 3.34; N, 24.29; Co, 10.21. $C_{14}H_{20}CoN_{10}O_{12}$ requires C, 29.03; H, 3.48; N, 24.18; Co, 10.17%. FT-IR ν_{max}(KBr pellet)/cm^{-1}: 3434s ν(O−H); 3271s (ν(NH$_2$) + 2δ(NH$_2$)); 3077s, 2889m (ν(C$_8$−H + C$_2$−H) +(ν(NH$_2$)); 1695s ν_{as}(O−C−O); 1630vs, 1613vs (ν(C═C) + δ(NH$_2$)); 1550s ν((C$_4$−C$_5$) + (N$_3$−C$_4$−C$_5$)); 1435s (δ(C$_2$−H + C$_8$−N$_9$) + ν(C$_8$−H)); 1404sh δ(N$_1$−C$_6$−H$_6$); 1378s ν(C$_5$−N$_7$−C$_8$); 1300s (ν(N$_9$−C$_8$ + N$_3$−C$_2$) + δ(C−H) + ν_s(O−C−O)); 1228m, 1212sh, 1152w, 1117w (δ(C$_8$−H) + ν(N$_7$−C$_8$)); 1020w, 998w τ(NH$_2$); 952w, 902 m (ν(N$_1$−C$_6$) + τ-(NH$_2$)); 782m δ(O−C−O); 712m, 683sh, 618m (ring deformation); 533m, 490m ν(M−O).

(3*H*,7*H*-ade)$_2$[Zn(ox)$_2$(H$_2$O)$_2$]·2H$_2$O (3). The synthesis for compound **3** is similar to that described for **2** but replacing [Co-(μ-ox)(H$_2$O)$_2$] for [Zn(μ-ox)(H$_2$O)$_2$] (0.027 g, 0.14 mmol). Likewise, after acidification with $H_2C_2O_4$, a white powder precipitates, and colorless X-ray quality single crystals are obtained by evaporation from the mother liquid (pH 4.5). Yield: 30−40%. Found: C, 28.78; H, 3.35; N, 23.90; Zn, 11.21. $C_{14}H_{20}N_{10}O_{12}Zn$ requires C, 28.71; H, 3.44; N, 23.91; Zn, 11.16%. FT-IR ν_{max}(KBr pellet)/cm^{-1}: 3440s ν(O−H); 3280s (ν(NH$_2$) + 2δ(NH$_2$)); 3076s, 2889s (ν(C$_8$−H + C$_2$−H) +(ν(NH$_2$)); 1694s ν_{as}(O−C−O); 1639vs, 1614vs (ν(C═C) + δ(NH$_2$)); 1551s ν((C$_4$−C$_5$) + (N$_3$−C$_4$−C$_5$)); 1433s (δ(C$_2$−H + C$_8$−N$_9$) + ν(C$_8$−H)); 1404sh δ(N$_1$−C$_6$−H$_6$); 1378s ν(C$_5$−N$_7$−C$_8$); 1302s (ν(N$_9$−C$_8$ + N$_3$−C$_2$) + δ(C−H) + ν_s(O−C−O)); 1228m, 1209sh, 1149w, 1118w (δ(C$_8$−H) + ν(N$_7$−C$_8$)); 1018w, 1002w τ(NH$_2$); 953m, 900s (ν(N$_1$−C$_6$) + τ(NH$_2$)); 782m δ(O−C−O); 711m, 683m, 617s (ring deformation); 531m, 492m ν(M−O).

X-ray Data Collection and Structure Determination. Diffraction data were collected at 293(2) K on an Oxford Xcalibur diffractometer with graphite-monochromated Mo Kα radiation (λ = 0.71073 Å). The data reduction was done with the CrysAlis RED program.[25] Structures were solved by direct methods using the SIR 92 program[26] and refined by full-matrix least-squares on F^2 including all reflections (SHELXL97).[27] All calculations were

(25) *CrysAlis RED*, version 1.170; Oxford Diffraction: Wroclaw, Poland, 2003.
(26) Altomare, A.; Cascarano, M.; Giacovazzo C.; Guagliardi, A. *J. Appl. Crystallogr.* **1993**, *26*, 343.
(27) Sheldrick, G. M. *SHELXL97*; University of Göttingen: Göttingen, Germany, 1997.

performed using the WinGX crystallographic software package.[28] The final geometrical calculations and the graphical manipulations were carried out with the PARST95[29] and PLATON[30] programs. Crystal parameters and details of the final refinements of compounds **1**−**3** are summarized in Table 1. The labeling scheme used here for the adenine is that conventionally accepted for chemical and biological purposes.

Computational Details. All the quantum mechanical calculations of geometry optimization of the compounds and related models have been carried out in the gas phase using the density functional theory with Becke's three-parameter exchange functional[31] along with the Lee−Yang−Parr nonlocal correlation functional (B3LYP).[32] The standard 6-31G(d) basis set was used as implemented in the Gaussian03 program.[33] It is well-known that although the B3LYP functional method might not be suitable for the consistent study of the whole range of the DNA base interactions due to its insufficiency in describing the dispersion interactions, it predicts reliable interaction energies for hydrogen-bonded systems.[34] The initial geometry of the models was built from the experimental crystal structures. The solvation effect has been studied using the self-consistent reaction field (SCRF) method. In the Onsager model[35] the water is considered as a uniform dielectric with a dielectric constant $\epsilon = 78.5$. The spherical cavity size of radius a_0, where the solute is located, was calculated with the Volume keyword as implemented in Gaussian. The corresponding molecular radii, which had been increased by 0.5 Å to account for the nearest approach of solvent molecules, were used. The interaction energies were corrected for the basis set superposition error (BSSE) using the standard Boys−Bernardi counterpoise correction scheme.[36]

Results and Discussion

Description of the Structures. The supramolecular architecture of all compounds is quite similar, and their overall crystal packing can be regarded as a lamellar inorganic−organic hybrid network built up of anionic sheets of metal−oxalato−water complexes and cationic nucleobase layers among them (Figure 1). Each wide organic layer serves as "double-sided adhesive tape" to tightly join adjacent inorganic layers by means of electrostatic forces and a strong hydrogen-bonding network. The different protonation sites of the adenine nucleobase result in dissimilar hydrogen-bonding motifs between the structural units.

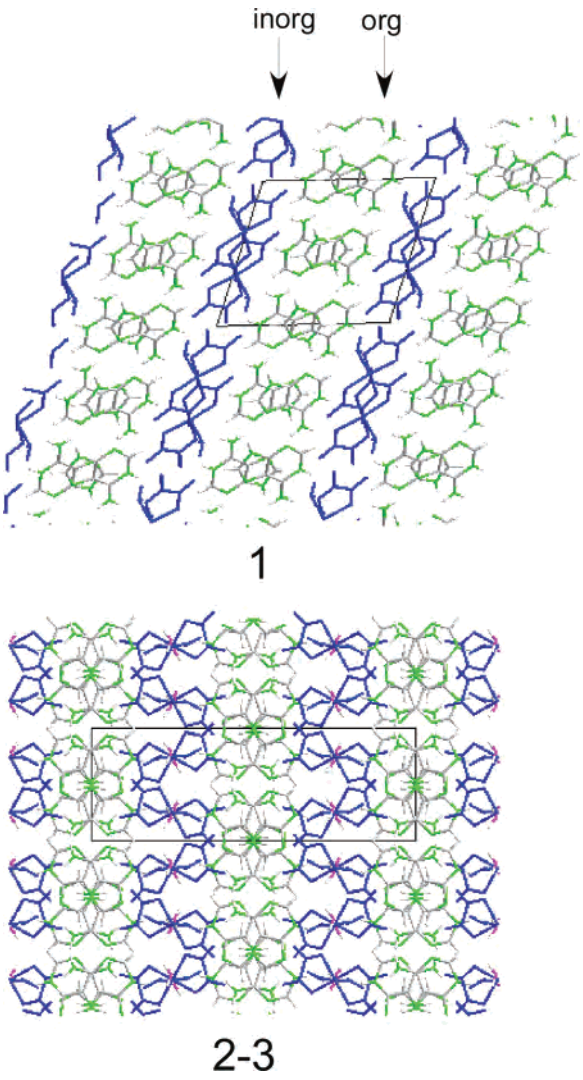

Figure 1. Crystal packing of compounds **1**−**3** showing the alternative inorganic−organic sheets.

(1*H*,9*H*-ade)$_2$[Cu(ox)$_2$(H$_2$O)] [1]. The asymmetric unit of **1** contains one oxalato-containing Cu(II) complex and two crystallographically independent adeninium cations (A and B) with protons at the N1 and N9 sites (Figure 2). Selected bond lengths and angles for the coordination polyhedron and structural parameters of the hydrogen bonding interactions of compound **1** are gathered in Table 2. The Cu(II) ion is coordinated by two chelating oxalate anions in a planar geometry (angle between the oxalato mean planes of ca. 1.21°), and the coordinated water molecule forms a long axial contact of 2.411(5) Å. These units dimerize through one of the coordinating O atoms of the oxalato [Cu1−O(22)^{i}: 3.024(5) Å] resulting in a Cu1···Cu1^{i} separation of 3.754-(3) Å [symmetry code: (i) $-x$, $1 - y$, $-z$]. The axial Cu−

(28) Farrugia, L. J. *WINGX, A Windows Program for Crystal Structure Analysis*; University of Glasgow: Glasgow, Great Britain, 1998.
(29) Nardelli, M. *J. Appl. Crystallogr.* **1995**, *28*, 659.
(30) Spek, A. L. *Acta Crystallogr.* **1990**, *A46*, 34.
(31) Becke, A. D. *J. Chem. Phys.* **1993**, *98*, 5648.
(32) (a) Lee, C.; Yang, W.; Parr, R. G. *Phys. Rev.* **1988**, *B37*, 785. (b) Miehlich, B.; Savin, A.; Stoll, H.; Preuss, H. *Chem. Phys. Lett.* **1989**, *157*, 2000.
(33) Frisch, M. J.; Trucks, G. W.; Schlegel, H. B.; Scuseria, G. E.; Robb, M. A.; Cheeseman, J. R.; Montgomery, J. A., Jr.; Vreven, T.; Kudin, K. N.; Burant, J. C.; Millam, J. M.; Iyengar, S. S.; Tomasi, J.; Barone, V.; Mennucci, B.; Cossi, M.; Scalmani, G.; Rega, N.; Petersson, G. A.; Nakatsuji, H.; Hada, M.; Ehara, M.; Toyota, K.; Fukuda, R.; Hasegawa, J.; Ishida, M.; Nakajima, T.; Honda, Y.; Kitao, O.; Nakai, H.; Klene, M.; Li, X.; Knox, J. E.; Hratchian, H. P.; Cross, J. B.; Bakken, V.; Adamo, C.; Jaramillo, J.; Gomperts, R.; Stratmann, R. E.; Yazyev, O.; Austin, A. J.; Cammi, R.; Pomelli, C.; Ochterski, J. W.; Ayala, P. Y.; Morokuma, K.; Voth, G. A.; Salvador, P.; Dannenberg, J. J.; Zakrzewski, V. G.; Dapprich, S.; Daniels, A. D.; Strain, M. C.; Farkas, O.; Malick, D. K.; Rabuck, A. D.; Raghavachari, K.; Foresman, J. B.; Ortiz, J. V.; Cui, Q.; Baboul, A. G.; Clifford, S.; Cioslowski, J.; Stefanov, B. B.; Liu, G.; Liashenko, A.; Piskorz, P.; Komaromi, I.; Martin, R. L.; Fox, D. J.; Keith, T.; Al-Laham, M. A.; Peng, C. Y.; Nanayakkara, A.; Challacombe, M.; Gill, P. M. W.; Johnson, B.; Chen, W.; Wong, M. W.; Gonzalez, C.; Pople, J. A. *Gaussian 03*, revision C.02; Gaussian, Inc.: Wallingford, CT, 2004.
(34) (a) Rappe, A. K.; Bernstein, E. R. *J. Phys. Chem. A* **2000**, *104*, 6117. (b) Sukhanov, O. S.; Shiskin, O. V.; Gorb, L.; Podolyan, Y.; Leszczynskii, J. *J. Phys. Chem. B* **2003**, *107*, 2846. (c) Morozov, A. V.; Kortemme, T.; Tsemekhman, K.; Baker, D. *Proc. Natl. Acad. Sci. U.S.A.* **2004**, *101*, 6946.
(35) (a) Onsager, L. *J. Am. Chem. Soc.* **1936**, *58*, 1486. (b) Wong, M. W.; Frisch, M. J.; Wiberg, K. B. *J. Am. Chem. Soc.* **1991**, *113*, 4776.
(36) (a) Janssen, H. B.; Ross, P. *Chem. Phys. Lett.* **1969**, *3*, 140. (b) Boys, S. F.; Bernardi, F. *Mol. Phys.* **1970**, *19*, 553.

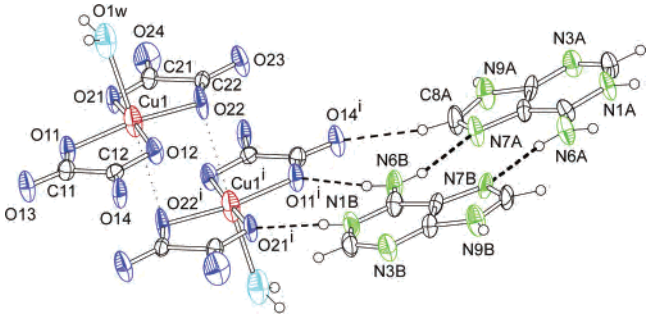

Figure 2. Perspective drawing of structural units of compound **1**. Displacement ellipsoids are drawn at the 50% probability level. Hydrogen bonds are shown as dashed lines. Symmetry code: (i) $-x$, $1-y$, $-z$.

O_{ox} bond distance exceeds the equatorial ones by ca. 1.0 Å, and the tetragonal parameter ($T = 0.65$) is significantly low, indicating that the axial oxygen atom is borderline to be considered as semicoordinated.[37] However, these values are similar to those reported in analogous oxalato−copper(II) complexes where the bridge group acts in a bidentate-monodentate bridging mode (μ-1,1,2-oxalato).[38]

The anionic complexes are joined by means of short hydrogen bonds O_{1w}-H···O_{ox} giving rise to sheets which spread out along the crystallographic *ab*-plane (Figure 3a). 1*H*,9*H*-Adeninium cations are inserted between the anionic sheets, and they are sequentially arranged to form polymeric ribbonlike 1D supramolecular aggregates (Figure 3b). These positively charged ribbons are substained by means of two different types of intermolecular interactions. The Hoogsteen faces (N6−H, N7) of two neighboring A and B adeninium cations are doubly N6−H···N7 hydrogen bonded to give a base pair (I), whereas the opposite faces of the dimeric aggregates are linked to the adjacent 1*H*,9*H*-ade$^+$ cations through one pair of N9−H···N3 hydrogen bonds in a R_2^2-(8) pattern (II),[39] which is a usual base-pairing mode found for adenine and its derivatives.[40,41] The other feasible dimeric adenine−adenine interaction[42] involving simultaneously two Watson−Crick faces is precluded in compound **1** by the protonation of the N1 site.

It should be emphasized that ribbon or layer arrangements of nucleobase pairs are common,[43] and both types of adeninium−adeninium self-association base pairs found in **1** are also suitable for adeninium−adenine and even adenine−adenine pairing. Indeed, the same pattern of ribbon structure has been found in the crystals of the (1*H*,9*H*-ade)$_2$SO$_4$·2H$_2$O[44] and (9*H*-ade)(1*H*,9*H*-ade)X·2H$_2$O (X = BF_4^-, ClO_4^-)[40,45] compounds, but we have only found one crystal structure in the crystallographic database of Cambridge (CSD, August 2006 release)[46] with ribbons consisting solely of neutral adenine molecules with both Watson−Crick and Hoogsteen faces involved in the hydrogen-bonding system within the ribbon.[47] Nevertheless, a similar spatial arrangement constructed out of dimers of neutral adenine molecules was used as the model for monolayers and bilayers deposited on graphite surfaces, studied by scanning tunneling microscopy, and for usually complicated superstructures of nucleic acid molecules (e.g., 1D filaments and 2D monolayers) formed at ultrahigh vacuum conditions on the Cu and Ag terminated Si surfaces, examined by the RAIRS method.[48]

In order to analyze the observed adeninium−adeninium interactions, B3LYP geometric optimizations have been performed on two dimeric models taken from the structural data and without any symmetry restraint (Figure 4). The optimized structure of interaction II shows very similar geometric parameters to the experimental ones except for the longer intermolecular distances (see Supporting Information). This fact can be explained on the basis of the electrostatic repulsive forces established between them, which are partially reduced in the crystal structure because of the anionic complex layers surrounding these cationic entities.

For the interaction involving the Hoogsteen edges (I), the main difference between the optimized structure parameters and the experimental ones is the non-coplanarity of the two adeninium molecules with an angle between the mean planes of ca. 33° and 3.4°, respectively (Figure 4a). This disposition is favored by the relative flexibility of the exocyclic amino group to rotate around the C−N bond. The rotation implies a decrease in the electron delocalization of the amino group into the aromatic system and, as a consequence, a slight pyramidalization of the exocyclic nitrogen atom, giving rise to a greater sp^3 character. Optimized structure provides evidence that this fact produces a decrease in the H−N−H angle and an increase in the C−N bond length. This non-coplanarity stabilizes the system by a larger mean distance between the two positively charged adeninium entities, and it improves the hydrogen-bonding parameters. However, a structural optimization of the interactions I and II for two neutral adenine molecules leads to similar values of the dihedral angles between the neutral nucleobases, suggesting that the key factor of the nonplanarity is the optimization of the hydrogen bonding interactions. A question arises when comparing this optimized structure with the experimental one: Why do the two adeninium cations remain coplanar in the crystal structure? An optimized linear tetrameric adeninium aggregate undergoes a similar nonplanarity around the interaction I, precluding a simple explanation based only

(37) Hathaway, J. *Struct. Bonding* **1984**, *55*, 55.
(38) (a) Keene, T. D.; Hursthouse, M. B.; Price, D. J. *Acta Crystallogr.* **2004**, *E60*, 378. (b) Castillo, O.; Luque, A.; Iglesias, S; Guzmán-Miralles, C.; Román, P. *Inorg. Chem. Commun.* **2001**, *4*, 640 and references therein.
(39) (a) Etter, M. C. *Acc. Chem. Res.* **1990**, *23*, 120. (b) Bernstein, J.; Davis, R. E.; Shimoni, L.; Chang, N. L. *Angew. Chem., Int. Ed. Engl.* **1995**, *34*, 1555.
(40) Cheng, Y. J.; Wang, Z. M.; Liao, C. S.; Yan, C. H. *New J. Chem.* **2002**, *26*, 1360.
(41) Young, A. C. M.; Dewan, J. C.; Edwards, A. J. *Acta Crystallogr.* **1991**, *C47*, 580.
(42) Kelly, R. E. A.; Lee, Y. J.; Kantorovich, L. N. *J. Phys. Chem. B* **2005**, *109*, 11933.
(43) *Hydrogen Bonding in Biological Structures*; Jeffrey, G. A., Sanger, W., Eds.; Springer-Verlag: Berlin, 1994.
(44) Langer, V.; Huml, K.; Lessinger, L. *Acta Crystallogr.* **1978**, *B34*, 2229.
(45) Zelenak, V.; Vargova, Z.; Cisarova, I. *Acta Crystallogr.* **2004**, *E60*, 742.
(46) Allen, F. H. *Acta Crystallogr.* **2002**, *B58*, 380.
(47) Dobrzynska, D.; Jerzykiewicz, L. B. *J. Am. Chem. Soc.* **2004**, *126*, 11118.
(48) (a) Kelly, R. E. A.; Kantorovich, L. N. *J. Mater. Chem.* **2006**, *16*, 1894. (b) Preuss, M.; Schmidt, W. G.; Bechstedt, F. *Phys. Rev. Lett.* **2005**, *94*, 236102. (c) Shinoda, K.; Shinoda, W.; Liew, C. C.; Tsuzuki, S.; Morikawa, Y.; Mikami, M. *Surf. Sci.* **2004**, *556*, 109. (d) McNutt, A.; Haq, S.; Raval, R. *Surf. Sci.* **2003**, *531*, 131.

Table 2. Selected Structural Parameters (Å, deg) for Compound **1**[a]

Cu−O(11)	1.917(4)	O(11)−Cu−O(12)	84.9(2)	O(12)−Cu−O(22)^{i}	84.0(2)
Cu−O(12)	1.943(4)	O(11)−Cu−O(21)	94.1(2)	O(21)−Cu−O(22)	86.3(2)
Cu−O(21)	1.914(4)	O(11)−Cu−O(22)	171.4(3)	O(21)−Cu−O(1w)	90.3(2)
Cu−O(22)	1.912(4)	O(11)−Cu−O(1w)	89.3(2)	O(21)−Cu−O(22)^{i}	90.0(2)
Cu−O(1w)	2.411(5)	O(11)−Cu−O(22)^{i}	87.8(2)	O(22)−Cu−O(1w)	99.2(2)
Cu···O(22)^{i}	3.024(5)	O(12)−Cu−O(21)	174.0(3)	O(22)^{i}−Cu−O(1w)	177.2(2)
Cu···Cu^{i}	3.754(3)	O(12)−Cu−O(22)	93.8(2)	O(22)−Cu−O(22)^{i}	83.6(2)
		O(12)−Cu−O(1w)	95.6(2)	Cu−O(22)−Cu^{i}	96.4(2)

D−H···A[b]	H···A	D···A	D−H···A
O(1w)−H(11w)···O(14)^{ii}	1.89	2.677(6)	152
O(1w)−H(12w)···O(24)^{iii}	2.03	2.780(6)	148
N(1A)−H(1A)···O(13)^{ii}	1.90	2.736(6)	163
N(6A)−H(62A)···O(12)^{ii}	2.08	2.911(6)	163
N(6A)−H(61A)···N(7B)^{iv}	2.12	2.959(6)	164
N(9A)−H(9A)···N(3B)	2.09	2.913(7)	161
N(1B)−H(1B)···O(21)^{v}	1.95	2.776(6)	159
N(6B)−H(61B)···O(11)^{v}	2.02	2.869(6)	168
N(6B)−H(62B)···N(7A)^{vi}	2.16	2.995(7)	164
N(9B)−H(9B)···N(3A)	2.17	2.990(7)	160
C(8A)−H(8A)···O(14)^{vii}	2.26	3.168(8)	164
C(2A)−H(2A)···O(23)^{iii}	2.29	3.037(9)	137
C(8B)−H(8B)···O(22)^{iii}	2.19	3.121(7)	175
C(2B)−H(2B)···O(1w)^{viii}	2.40	3.221(8)	148

[a] Symmetry codes: (i) $-x, 1-y, -z$; (ii) $-x, -y, -z$; (iii) $1-x, 1-y, -z$; (iv) $-1+x, -1+y, z$; (v) $2-x, 1-y, 1-z$; (vi) $1+x, 1+y, z$; (vii) $1-x, -y, 1-z$; (viii) $1+x, y, 1+z$. [b] D: donor. A: acceptor.

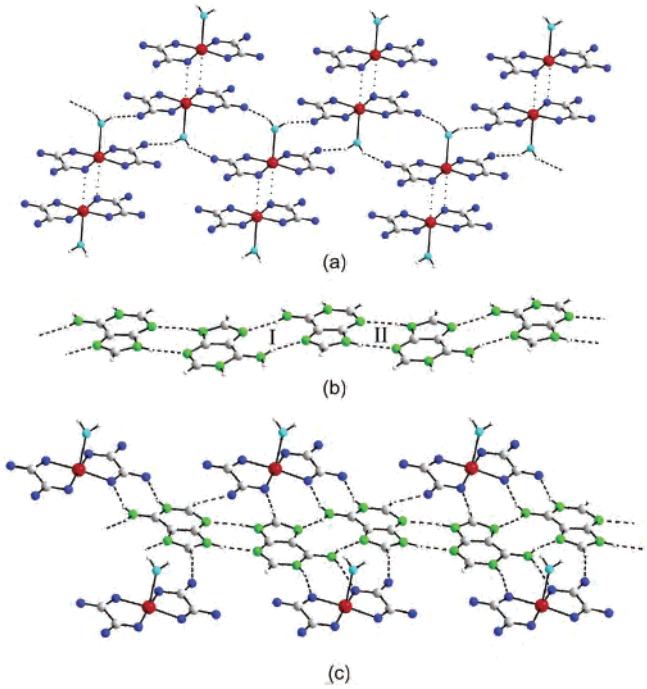

Figure 3. Ball and stick representation of (a) the inorganic sheets, (b) the one-dimensional adeninium chain, and (c) the inorganic−organic hydrogen bonding interactions in compound **1**.

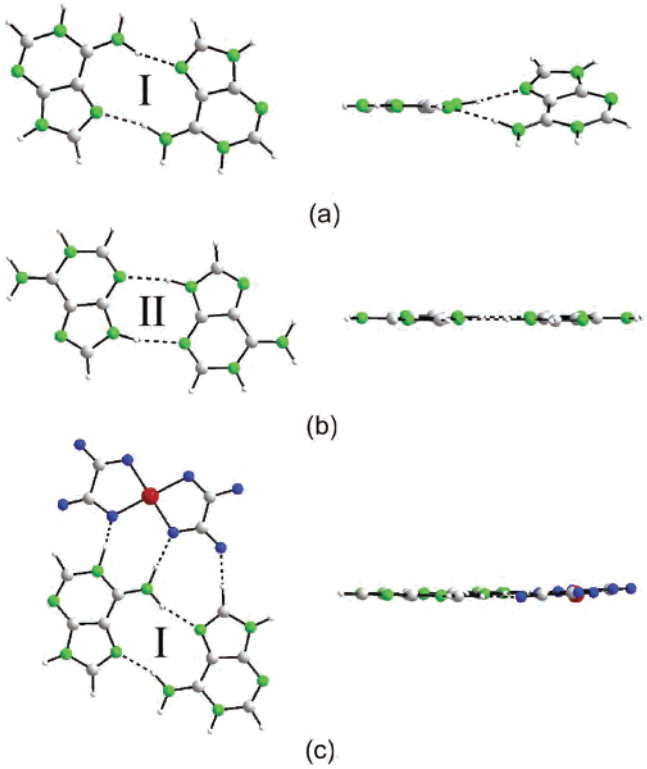

Figure 4. Frontal and lateral views of the optimized structure involving the interaction of two adeninium cations through the hydrogen-bonding patterns (a) I and (b) II, and (c) two cations with the metal−oxalato fragment.

on the interactions involved in the polymerization of the supramolecular adeninium chains.

In the crystal structure, the organic ribbons are connected to the complex entities containing copper through hydrogen bonds involving the Watson−Crick faces (N6H, N1H) of both adenine moieties as donors and the oxalato oxygen atoms as acceptors. Molecules A and B are engaged to O−C−O and O−Cu−O frameworks, respectively, leading to different $R_2^2(8)$ and $R_3^3(9)$ hydrogen-bond motifs in a clear example of a molecular recognition process which directs the supramolecular architecture of the compound (Figure 3c).

The interaction through the Watson−Crick edge imposes the planarity on the two donor groups, and therefore, no rotation of the amino group is allowed. A DFT optimization procedure of this adeninium−adeninium dimeric entity in the presence of an adjacent $[Cu(ox)_2]^{2-}$ fragment in the same disposition as found in the crystal structure has been carried out, and the result shows a planar arrangement of two adeninium cations with similar hydrogen-bond parameters to those experimentally found (see Supporting Information).

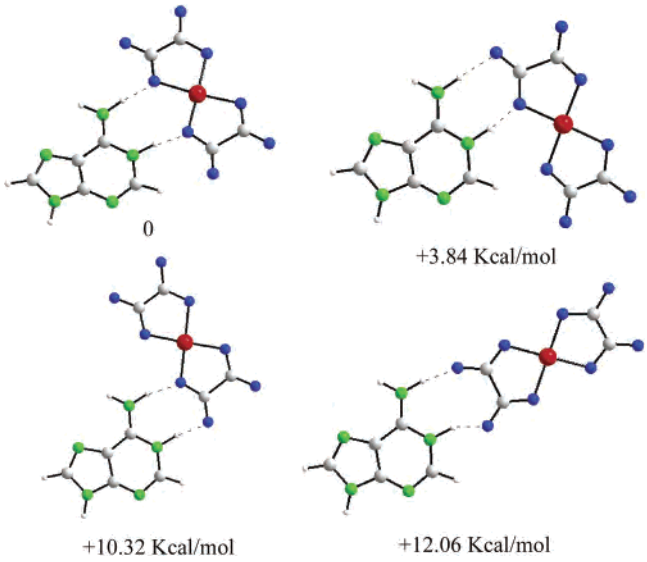

Figure 5. Most plausible interactions of the adeninium Watson−Crick edge with a metal−oxalato framework.

Therefore, it could be concluded that the key factor governing the planarity of the adeninium chains is the supramolecular recognition process with the surrounding inorganic sheets.

In order to get a deeper insight into the interaction of the 1*H*,9*H*-adeninium tautomer with a metal−oxalato fragment, we have optimized the most plausible arrangements between an adeninium cation and a $[Cu(ox)_2]^{2-}$ complex anion (Figure 5). The results indicate that interaction implying the Watson−Crick edge with the O−Cu−O fragment is the most favorable with an energy difference of 10.32 kcal/ mol with respect to that involving the O−C−O group with the observed arrangement in the experimental structure. The presence of the second type of interaction in the crystal packing can be attributable to the periodicity constraints of the anionic sheets.

Furthermore, the cohesiveness between the organic and inorganic layer is reinforced by weak C−H···O hydrogen bonds. Although hydrogen bonds concerning the C atom of the adenine did not use to be considered,[49] they may have biological relevance. Thereby, in the crystal structure of an alternating RNA octamer, the adenine bases form A*(G•C) base triples with C−H···N (guanine) hydrogen bonds.[50]

In conclusion, the supramolecular structure of **1** has been created by three types of molecular recognition: (a) between complex anions, (b) between adeninium cations, and (c) between ribbons of nucleobases and layers consisting of oxalato complexes. Molecules of complexes located within the parallel layers are joined by hydrogen bonds. The second interaction between the base molecules results in the double-faced hydrogen-bonding recognition unit and leads to the ribbon form. Finally, the third group of hydrogen bonds completes the very effective set of interactions and builds the closely packed structure.

(3*H*,7*H*-ade)$_2$[M(ox)$_2$(H$_2$O)$_2$]·2H$_2$O [M(II) = Co(2) and Zn(3)]. The crystal structures of compounds **2** and **3** consist of centrosymmetric complex anions $[M(ox)_2(H_2O)_2]^{2-}$, 3*H*,7*H*-adeninium cations, and crystallization water molecules linked together by electrostatic interactions and an intricate network of hydrogen bonds. A perspective view of the structural units of compound **2**, with the atomic numeric scheme, is given in Figure 6. Main bond lengths and angles together with the structural parameters of the hydrogen-bond interactions are listed in Table 3. The coordination polyhedron of the metal atom is an octahedron with an equatorial plane formed by four oxygen atoms from two bidentate oxalato ligands and with water molecules in the axial sites to give a $O_4(O_w)_2$ donor set. The equatorial chelate rings are nearly planar, and the M−Ow axial bonds are perpendicular to them. The M−Ow axial bonds [2.101(3) Å for **2** and 2.153(2) Å for **3**] are longer than the equatorial bonds [<2.09 Å] in good agreement with the axial elongation found in other *trans*-diaquabis(oxalato-*O*,*O*')metalate complexes.[51]

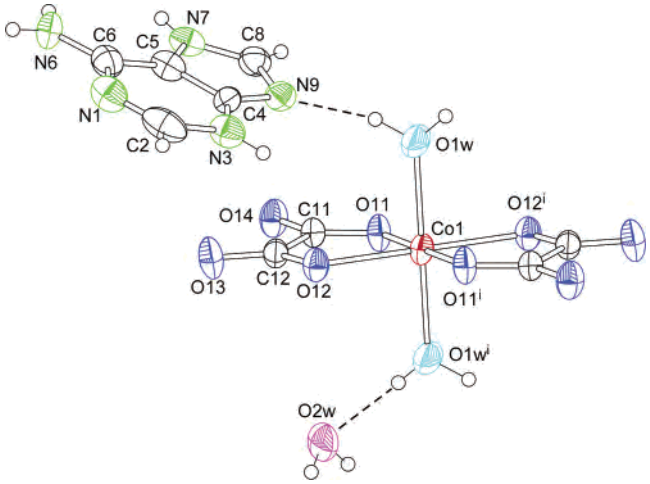

Figure 6. ORTEP view of the structural units of compound **2** showing the labeling scheme. Symmetry code: (i) $^1/_2 - x$, $^3/_2 - y$, $1 - z$.

Crystallization water molecules occupy the interstitial space between the anionic complexes and display hydrogen contacts to the coordinated ones and to the oxalato oxygen atoms to form anionic inorganic sheets spreading along the *bc*-plane (Figure 7). Chains of adeninium cations running along the crystallographic *b*-axis are inserted among the anionic sheets to give an inorganic−organic layered structure.

The nucleobase cations undergo association through intermolecular hydrogen bonding between the C8H proton of an adeninium entity and the deprotonated N1 position of the adjacent one, leading to infinitely long ribbons in which the adenine bases are coplanar. Intermolecular hydrogen bond formation between CH groups of nucleobases and endocyclic N atoms is common in synthetic systems, but it is still extremely rare in nucleic acid chemistry.[50] Moreover, in both artificial and natural structures, the weak C−H···N interbase interactions usually reinforce strong neighboring N−H···N/O hydrogen bonds, but an analysis of the contacts in **2** and **3** reveals that the almost linear C8−H···N1 hydrogen bond is

(49) Amo-Ochoa, P.; Sanz-Miguel, P. J.; Lax, P.; Alonso, I.; Roitzsch, M.; Zamora, F.; Lippert, B. *Angew. Chem., Int. Ed.* **2005**, *44*, 5670.
(50) Shi, K.; Biswas, R.; Nath Mitra, S.; Sundaralingam, M. *J. Mol. Biol.* **2000**, *299*, 113.
(51) Román, P.; Guzmán-Miralles, C.; Luque, A. *Acta Crystallogr.* **1993**, *C49*, 1336.

Table 3. Selected Structural Parameters (Å, deg) for Compounds **2** and **3**[a]

Compound **2**

Co−O(11)	2.079(3)	O(11)−Co−O(11)^{i}	180.0(−)	O(11)−Co−O(1w)	90.2(1)
Co−O(12)	2.085(3)	O(12)−Co−O(12)^{i}	180.0(−)	O(11)−Co−O(1w)^{i}	89.8(1)
Co−O(1w)	2.101(3)	O(11)−Co−O(12)	80.4(1)	O(12)−Co−O(1w)	92.7(1)
		O(11)−Co−O(12)^{i}	99.6(1)	O(12)−Co−O(1w)^{i}	87.3(1)
				O(1w)−Co−O(1w)^{i}	180.0(−)

D−H···A[b]	H···A	D···A	D−H···A
O(1w)−H(12w)···O(2w)^{i}	2.09	2.923(5)	178
O(1w)−H(11w)···N(9)	1.89	2.742(5)	164
N(3)−H(3)···O(2w)^{ii}	2.04	2.890(6)	169
N(6)−H(6A)···O(13)^{iii}	2.02	2.858(5)	166
N(6)−H(6B)···O(14)^{iv}	1.97	2.827(5)	176
N(7)−H(7)···O(13)^{iii}	1.97	2.761(6)	152
N(7)−H(7)···O(14)^{iii}	2.25	2.875(5)	129
O(2w)−H(21w)···O(12)^{v}	1.94	2.836(5)	169
O(2w)−H(22w)···O(11)^{vi}	2.28	3.122(5)	173
C(8)−H(8)···N(1)^{vii}	2.32	3.213(7)	162
C(2)−H(2)···O(1w)^{viii}	2.60	3.532(8)	175

Compound **3**

Zn−O(11)	2.062(2)	O(11)−Zn−O(11)^{i}	180.0(−)	O(11)−Zn−O(1w)	90.32(9)
Zn−O(12)	2.067(2)	O(12)−Zn−O(12)^{i}	180.0(−−)	O(11)−Zn−O(1w)^{i}	89.68(9)
Zn−O(1w)	2.153(2)	O(11)−Zn−O(12)	81.81(7)	O(12)−Zn−O(1w)	92.46(9)
		O(11)−Zn−O(12)^{i}	98.19(7)	O(12)−Zn−O(1w)^{i}	87.54(8)
				O(1w)−Zn−O(1w)^{i}	180.0(−)

D−H···A[b]	H···A	D···A	D−H···A
O(1w)−H(12w)···O(2w)^{i}	2.11	2.914(3)	178
O(1w)−H(11w)···N(9)	1.92	2.762(3)	166
N(3)−H(3)···O(2w)^{ii}	2.02	2.871(4)	168
N(6)−H(6A)···O(13)^{iii}	2.01	2.849(3)	166
N(6)−H(6B)···O(14)^{iv}	1.98	2.840(3)	176
N(7)−H(7)···O(13)^{iii}	1.98	2.767(4)	152
N(7)−H(7)···O(14)^{iii}	2.26	2.880(3)	129
O(2w)−H(21w)···O(12)^{v}	1.94	2.833(3)	170
O(2w)−H(22w)···O(11)^{vi}	2.27	3.122(3)	172
C(8)−H(8)···N(1)^{vii}	2.33	3.225(5)	162
C(2)−H(2)···O(1w)^{viii}	2.59	3.517(5)	174

[a] Symmetry codes: (i) $^{1}/_{2} - x$, $^{3}/_{2} - y$, $1 - z$; (ii) x, $1 - y$, $^{1}/_{2} + z$; (iii) $-x$, y, $^{1}/_{2} - z$; (iv) $-x$, $-1 + y$, $^{1}/_{2} - z$; (v) $^{1}/_{2} - x$, $^{1}/_{2} + y$, $^{1}/_{2} - z$; (vi) $^{1}/_{2} - x$, $-^{1}/_{2} + y$, $^{1}/_{2} - z$; (vii) x, $1 + y$, z; (viii) x, $-1 + y$, z. [b] D: donor. A: acceptor.

the only one between neighboring adeninium cations, and their structural parameters (Table 3) indicate a relative strong interaction with values clearly below the ranges found for this structural motif in crystal structures retrieved from the CSD database.[46] All the remaining donor and acceptor sites of the nucleobases are engaged in hydrogen-bond formation between the ribbons and the inorganic sheets (Figure 7c).

One of the interesting structural aspects of compounds **2** and **3** is the protonation of the nucleobase in the N7 and N3 sites. The modest quality of the single crystals has precluded the localization of the adenine hydrogen atoms in the difference Fourier synthesis map, but the assignment of the protons has been unambiguously substantiated by the particular pattern of the hydrogen-bonding interactions. The N7-H is hydrogen bonded to two noncoordinated oxygen atoms from one oxalato ligand, whereas the N3 atom is close to the crystallization water molecule whose hydrogen atoms are attached to two oxalato oxygen atoms.

It is well-documented that the N9H amine form of adenine is the most stable in gas phase and water solution (pK_a = 9.8). This canonical tautomeric form contains three basic nitrogen atoms: the most basic site (pK_a = 4.2), which accepts the first proton, is N1, the next protonation occurs at N7, and then at N3. This situation is reflected by the available X-ray structures in the crystallographic CSD database containing free adenine (without metal coordination) as neutral or cationic entity. The proton is attached to the most basic N9 site in the great majority of the retrieved compounds, and the usual cationic species are the 1*H*,9*H*- and 1*H*,7*H*,9*H*-adeninium forms (see Supporting Information). Nevertheless, the minor N7H and N3H amino tautomers have larger dipole moments (more than 4.0 D)[52] than that found for the canonical N9H form (2.8 D),[19] and previous work has unequivocally established that hydration, as well as bulk water, stabilizes the minor tautomers, leading to the coexistence of the canonical and noncanonical forms in water solution and biological systems.[10a,53] On the basis of these data, it is not surprising that unusual tautomers and their protonated forms may be stabilized in the solid state by properly positioned hydrogen-bonding donor−acceptors. Indeed, in a previous work, our research group achieved the stabilization of the noncanonical 7*H*-amino tautomer by a manganese−oxalato−water framework, and the twofold 1*H*,7*H*-protonated form has been found in the crystals

(52) Laxer, A.; Major, D. T.; Gottlieb, H. E.; Fischer, B. *J. Org. Chem.* **2001**, *66*, 5463.
(53) Gu, J.; Leszczynski, J. *J. Phys. Chem. A* **1999**, *103*, 2744.

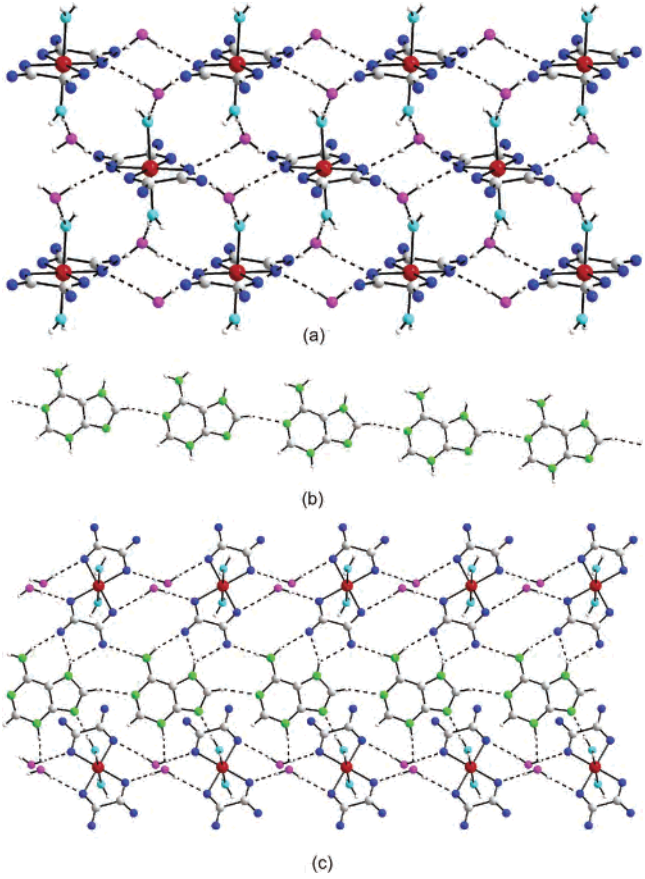

Figure 7. Ball and stick representation of (a) the inorganic sheets, (b) the one-dimensional adeninium chain, and (c) the inorganic−organic hydrogen-bonding interactions in compounds **2** and **3**.

(1*H*,7*H*-ade)$_2$(I$_3$)$_2$(I$_2$)$_5$(H$_2$O)$_2$,[54] (1*H*,7*H*-ade)$_4$(calix)·14H$_2$O (calix = *p*-sulfonatocalix(4)arene),[55] and (1*H*,7*H*-ade)$_2$Cl[ZnCl$_3$(1*H*,9*H*-ade-*kN*7)]·H$_2$O.[56] So, the 3*H*,7*H*-adenium cation in the crystal structure of compounds **2** and **3** can be described as a protonated form of the 7*H*-adenine tautomer.

Previous reports on gas-phase ab initio quantum mechanical calculations have determined that the energy order of the low lying tautomers is 1*H*,9*H*- < 3*H*,7*H*- < 3*H*,9*H*- < 7*H*,9*H*- < 1*H*,7*H*-, with a very small energy difference of 0.46 kcal/mol between the 1*H*,9*H*- and 3*H*,7*H*-adeninium form.[23] However, this noncanonical tautomer is unprecedented in nucleobase solid-state chemistry so far. Indeed, since the N3 site of the adenine is known to be the least basic relative to protonation, adenine moieties carrying proton at the N3 site are rare, and it has been solely observed in the crystal structure of the dimer (μ-ade-κ^2*N*7,*N*9)[Cu(H$_2$O)(bzimdi)]$_2$[18b] and in several *N*7-[57] and *N*6-gathered adenine species.[58]

In order to verify the feasible stabilization of noncanonical forms of the protonated adenine nucleobase, we have

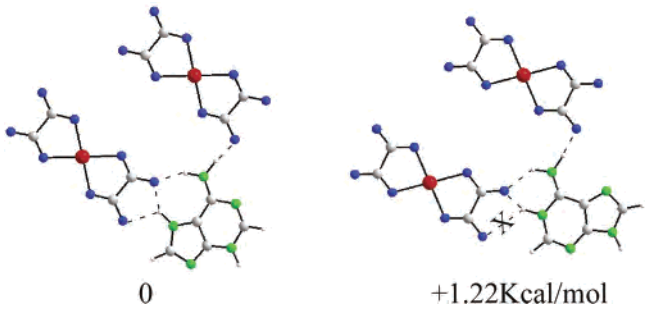

Figure 8. Hydrogen-bonding interactions for the optimized 3*H*,7*H*- and 1*H*,9*H*-adeninium-2[Cu(ox)$_2$]$^{2-}$ systems.

extended our B3LYP/6-31G(d) calculations to the study of the tautomeric forms of isolated cations on a water simulated dielectric medium and including different metal−oxalato surroundings simulating those experimentally found in the compounds.

The dielectric media of the solvent slightly stabilizes the 1*H*,9*H*-form with a difference of 0.52 kcal/mol with respect to the 3*H*,7*H*-adeninium cation. This stabilization is more pronounced for the 1*H*,7*H*-tautomer for which the gap energy, 4.41 kcal/mol, is substantially smaller than that found in the gas phase (10.87 kcal/mol) owing to its higher dipole moment. The high dipole moment enables it to establish strong noncovalent interactions with good hydrogen bonding donors/acceptors that could stabilize this tautomeric form such as has been observed in the crystal structure of the above-mentioned (1*H*,7*H*-ade)$_2$(I$_3$)$_2$(I$_2$)$_5$(H$_2$O)$_2$, (1*H*,7*H*-ade)$_4$(calix)·14H$_2$O, and (1*H*,7*H*-ade)$_2$Cl[ZnCl$_3$(1H,9H-ade-*kN*7)]·H$_2$O compounds.

On the other hand, the arrangement of adjacent hydrogen bond donor/acceptor sites surrounding the adenine moiety constrains the hydrogen-bonding pattern and, therefore, the protonation sites of the nucleobase (Scheme 3). The Watson−Crick and Hoogsteen edges of the 1*H*,7*H*-tautomer are protonated whereas the N3/N9 edge acts as a double acceptor group. In contrast, the 1*H*,9*H*- and 3*H*,7*H*-adeninium cations (with a quite similar donor/acceptor disposition) exhibit one double hydrogen bonding donor edge, the Watson−Crick face (N1−H/N6−H) for the former and Hoogsteen face (N6−H/N7−H) for the second one, and the remaining two edges act both as donor and acceptor sites. As a consequence of the different hydrogen-bonding pattern of the 1*H*,7*H*-tautomer with respect to those of 1*H*,9*H*- and 3*H*,7*H*-adeninium forms, it could be the preferred option for some environments, but a not extremely rigid supramolecular environment well designed to interact with the 3*H*,7*H*-tautomer will also be appropriate for the 1*H*,9*H*-form. As this latter tautomer is the most stable one and presents a slightly higher dipole moment, it would be the preferred one.

Calculations including the presence of one [Cu(ox)$_2$]$^{2-}$ fragment in all of its possible dispositions around the adeninium cation show that the energy order of 1*H*,9*H*- and 3*H*,7*H*-tautomers is not altered. However, when two [Cu(ox)$_2$]$^{2-}$ fragments with the experimental disposition of compound **2** are included, the 3*H*,7*H*-adeninium cation becomes the most stable. This fact is due to the demanding conditions for an efficient hydrogen-bonding interaction that

(54) Wang, Z.; Cheng, Y.; Liao, C.; Yan, C. *CrystEngComm* **2001**, *50*, 1.
(55) Atwood, J. L.; Barbour, L. J.; Dawson, E. S.; Junk, P. C.; Kienzle, J. *Supramol. Chem.* **1996**, *7*, 271.
(56) Taylor, M. R.; Westphalen, J. A. *Acta Crystallogr.* **1981**, *A37*, 63.
(57) Price, C. L.; Taylor, M. R. *Acta Crystallogr.* **1996**, *C52*, 2736.
(58) (a) Travnicek, Z.; Klanicova, A.; Popa, I.; Roicik, J. *J. Inorg. Biochem.* **2005**, *99*, 776. (b) Travnicek, Z.; Popa, I.; Dolezal, K. *Acta Crystallogr.* **2004**, *C60*, 662. (c) Stanley, N.; Muthiah, P. T.; Geib, S. J. *Acta Crystallogr.* **2003**, *C59*, 27.

Scheme 3

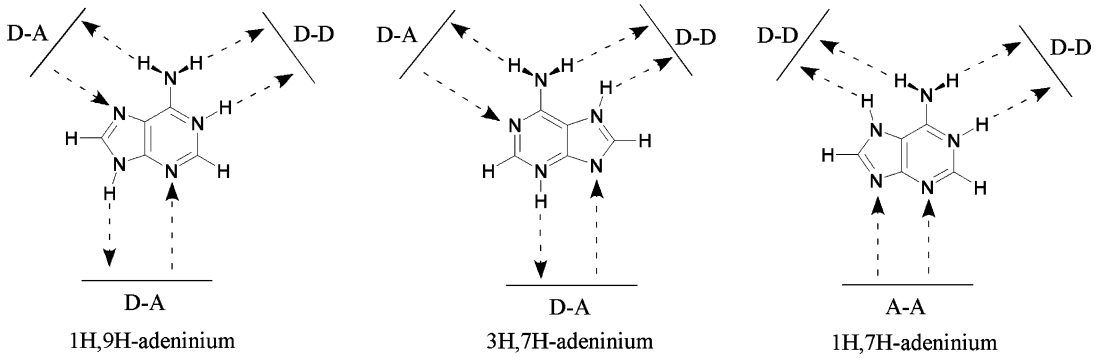

are better fulfilled by the 3*H*,7*H*-adeninium cation than by the 1*H*,9*H*-form. The optimized structural parameters of the hydrogen bonds around the 3*H*,7*H*-adeninium entity agree well with those obtained from the X-ray diffraction analysis, and they are within the range usually found for N−H···O hydrogen bonds. The optimized 1*H*,9*H*-adeninium entity establishes three hydrogen bonds with the $[Cu(ox)_2]^{2-}$ fragments (Figure 8), but the parameters of the fourth hydrogen bond involving the remaining oxygen atom of the first monomer are clearly outside the usual values, indicating a less efficient hydrogen-bonding stabilization for this tautomer (see Supporting Information).

Conclusion

In conclusion, we have isolated and structurally characterized three new M(II)−oxalato complexes containing the adeninium nucleobase. Depending on the chemical environment, different tautomers appear on the crystal structure. The canonical 1*H*,9*H*-adeninium tautomer is the most commonly found in the literature, and the isolation of other tautomeric forms requires specific chemical environments, as shown by means of the performed quantum mechanical calculations. The first solid-state characterized 3*H*,7*H*-adeninium tautomer requires an extremely rigid supramolecular environment to appear, since its hydrogen-bonding donor/acceptor arrangement is very similar to that of the 1*H*,9*H*-adeninium tautomer. The next stage of this work should employ other nucleobases in order to demonstrate the efficiency of the metal−oxalate matrix to embed supramolecular nucleobase architectures. This work contributes to a further understanding of the tautomeric and protonation equilibria of nucleobases and is therefore relevant to biological inorganic chemistry.

Acknowledgment. This work was supported by the Ministerio de Ciencia y Tecnología (MAT2005-03047) and the Universidad del País Vasco/Euskal Herriko Unibertsitatea (9/UPV 00169.310-15329/2003). J.P.G.-T. thanks Eusko Jaurlaritza/Gobierno Vasco for a predoctoral fellowship. The SGI/IZO-SGIker UPV/EHU (supported by the National Program for the Promotion of Human Resources within the National Plan of Scientific Research, Development and Innovation, Fondo Social Europeo and MCyT) is gratefully acknowledged for generous allocation of computational resources.

Supporting Information Available: X-ray crystallographic files in CIF format, usual protonation sites of the adenine for compounds compiled in the CSD database, and structural parameters for the DFT optimized structures of the isolated adenine tautomer and the models with the hydrogen-bonding environment found in compounds **1**−**3**. This material is available free of charge via the Internet at http://pubs.acs.org.

IC062448S